Variation of Effective Adsorbed Polymer Layer Thickness with Molecular Weight in Good and Poor Solvents

Jacob Klein*† and Paul F. Luckham‡

Polymer Department, Weizmann Institute of Science, Rehovot 76100, Israel, and Department of Chemical Engineering and Chemical Technology, Imperial College, London SW7, England. *Received January 7, 1986*

ABSTRACT: The variation of the effective adsorbed layer thickness δ_{eff} with molecular weight M for a polymer adsorbed at a mica–solvent interface under good solvent conditions, as revealed by force measurements, is analyzed. The observed variation, $\delta_{eff} \propto M^{0.43}$, is shown to be consistent with a scaling form for the extension of the polymer from the surface. The corresponding effective thickness of adsorbed layers in poor solvents is briefly considered.

Polymers adsorbed on solid surfaces immersed in a liquid medium may considerably change the surface characteristics; in particular they may lead to a strong modification of the long-range interaction forces between two surfaces bearing such adsorbed layers (relative to "bare" surface–surface interactions), an effect frequently used to stabilize (or destabilize) colloidal dispersions.[1] The conformation of adsorbed polymer layers has been extensively studied, using a variety of techniques, including macroscopic flow methods,[2,3] optical techniques,[4,5] disjoining pressure measurements,[6,7] and neutron scattering.[8,9] Except for the last mentioned, these methods generally yield a mean value for the adsorbed layer thickness (such as hydrodynamic thickness, in the case of flow experiments) that depends to some extent on the method used; neutron scattering can in principle be used to extract a segmental concentration profile of the adsorbed layer, through only a few studies have been reported.

Over the past few years we have studied the interaction between two smooth solid (mica) surfaces bearing adsorbed polymers in a liquid medium.[10–13] Our experiments measure the force $F(D)$ between two surfaces a distance D apart; at large D there is no measurable force between the surfaces, but, as they approach, interaction is eventually detected at separations $D < D_0$, where D_0 is an "onset-of-interaction" separation whose value depends on the polymer–solvent system used and on the size of the polymer. A characteristic effective layer thickness $\delta_{eff} = {}^1/_2 D_0$ can thus be evaluated, "effective" in the sense that is represents the range of extension from the surface that may be detected by a similar polymer-covered surface. As this is relevant in phenomena involving steric stabilization by adsorbed polymers, it is of interest how this effective thickness varies with the size of polymer used.

We have recently studied force-distance profiles between mica sheets with adsorbed polymers in two polymer–good solvent systems, poly(ethylene oxide) (PEO) in 0.1 M aqueous KNO_3 solution,[11,12] and PEO in toluene.[13] The characteristics of polymers used and the values of D_0 are summarized in Table I, taken from ref 11–13.

The results are shown on a log δ_{eff} vs. log(molecular weight) plot in Figure 1. The main feature is that the effective extension of the adsorbed layers varies as

$$\delta_{eff} \propto N^{\beta} \tag{1}$$

(where N is the degree of polymerization) in the range of molecular sizes used, where $\beta = 0.43 \pm 0.02$ for both systems studied. We have used a power-law representation of the data in eq 1 to highlight the difference between the variation of δ_{eff} with N and the assumed variation with N of the extension from the surface δ_{tail} of the "tails" of adsorbed polymer layers. The latter has often been taken as[15]

$$\delta_{tail} \propto R_F \sim N^{3/5} \tag{2}$$

(where R_F is the Flory radius) in good solvent conditions. If the onset of repulsive (osmotic) interactions between two adsorbed polymer layers in a good solvent occurs as soon as the respective "tails" (or distal segments) of each layer come into overlap, one wouuld expect $\delta_{eff} \simeq \delta_{tail}$. The results (compare eq 1 and 2) show that this is clearly not so.

Table I
Molecular Weight M and Interaction Onset Separation D_0 for PEO Adsorbed on Mica in Good Solvents[a]

M_w	solvent	M_w/M_n	R_0, nm	D_0, nm
4×10^4	0.1 M aqueous	1.03	16	46
1.6×10^5	KNO_3	1.04	32	80
1.2×10^6		1.12	86	190
4×10^4	toluene	1.03	16	58
1.6×10^5		1.04	32	110
3.1×10^5		1.05	44	135

[a] The molecular weights were determined by light scattering and gel permeation chromatography and supplied by the makers, Toyo Soda Co. (Japan). R_0 are the unperturbed end-to-end dimensions of the coils.[14]

In a recent study[4,5] Kawaguchi and co-workers measured the ellipsometric thickness δ_{ell} of adsorbed polymer layers on plane surfaces immersed in good solvents and found $\delta_{ell} \propto N^{0.4}$, a variation similar to that indicated by our results (eq 1). They explained their experimental result by assuming that (i) the adsorbed polymer layer extended to a thickness $\sim R_F$ from the adsorbing substrate, (ii) over this thickness the segmental density profile $\phi(z)$ at extensions z from the surface varied according to the de Gennes scaling proposal[15]

$$\phi(z) \sim z^{-4/3}$$

and (iii) their measured ellipsometric thickness was a measure of the first moment of the distribution

$$\delta_{ell} = \int_0^{R_F} z\phi(z)\, dz \sim N^{2/5} \tag{3}$$

However, this argument is clearly not applicable to our experiments, where we expect the distance for *onset* of interaction $D_0 = 2\delta_{eff}$ to be determined only by overlap of the distal segments and not to involve the whole profile.

Some insight into the behavior indicated in Figure 1 (and eq 1) is obtained by recalling that in the force measurement studies the *onset* of interaction is indicated when the force $F(D)$ between the polymer-bearing mica surfaces

† Weizmann Institute of Science.
‡ Imperial College.

0024-9297/86/2219-2007$01.50/0

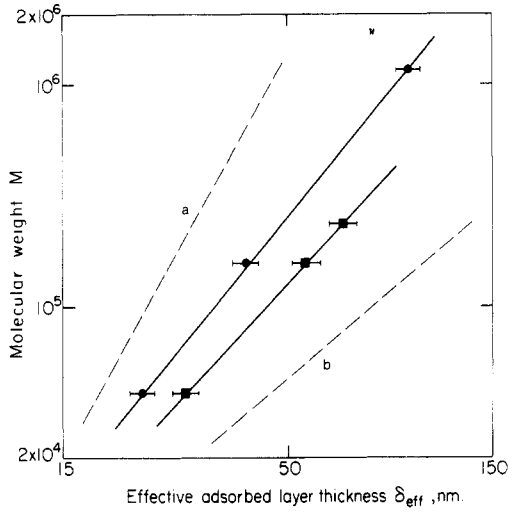

Figure 1. Variation (on a log–log plot) of the effective adsorbed layer thickness δ_{eff} with molecular weight M for PEO adsorbed onto mica from good solvents—0.1 M KNO_3 and toluene. δ_{eff} is evaluated as $^1/_2D_0$, where D_0 is the intersurface separation when interaction between the mica sheets is first detected, taken from force–distance measurements ((●) from ref 11 and 12, (■) from ref 13). The broken lines show for comparison slopes corresponding to (a) $\delta_{eff} \propto M^{0.3}$; (b) $\delta_{eff} \propto M^{0.6}$ (cf. eq 12 and 14).

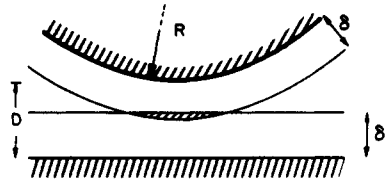

Figure 2. Schematic section through the crossed cylinder configuration of the mica sheets in the force–distance experiments of ref 11–13. δ represents the "true" extension of each adsorbed layer, D represents the distance of closest approach, and the central shaded lens has a volume V (eq 4).

equals the *detection limit* F^* of the experiment; i.e., whenever

$$F(D_0) = F^* \tag{3}$$

The geometry of the system is indicated in Figure 2, where the overlapping adsorbed layers form a "lens" of volume

$$V = \pi R(\delta - D/2)^2 \tag{4}$$

where R is the radius of the curved surfaces and δ the "true" extension from each surface of the adsorbed polymer layers (Figure 2). Making the first-order approximation that the volume fraction of polymer in the overlap "lens" has an effective mean value

$$\phi_0 = \phi(z)|_{z=D/2} \tag{5}$$

gives the total repulsive osmotic interaction energy due to overlap of segments in the "lens" as

$$E(D) \simeq V\phi_0^{9/4}kT/a^3 \tag{6}$$

where a^3 is a monomer volume and we assume the semidilute relation for osmotic pressure in a good solvent; i.e., we take $\phi_0 > \phi^*$, as the overlap concentration.[16] The *force* between the surfaces at D is

$$F(D) = \partial E(D)/\partial D \tag{7}$$

so that

$$F^* = \partial E(D)/\partial D|_{D=D_0} \tag{8}$$

Finally, we use the de Gennes relation[15] for polymer volume fraction $\phi(z)$ a distance z from the surface

$$\phi(z) = \phi_s(a/z)^{4/3} \tag{9}$$

where ϕ_s is the volume fraction of polymer at the surface ($z = a$).[17] From eq 4–9 we find

$$\frac{kT}{2a^3}\phi_s^{9/4}\pi R\left(\frac{2a}{D_0}\right)^3(2\delta - D_0)\left\{1 + \frac{3}{2}\frac{(2\delta - D_0)}{D_0}\right\} = F^* \text{ (a constant)} \tag{10}$$

This expression has two limits, depending—self-consistently—on the sensitivity of the experiment, that is, the magnitude of F^*: (i) For $F^* \to 0$ (extreme sensitivity of detection) we expect forces to be measurable (i.e., $D = D_0$) already at very little overlap of opposing layers (Figure 2)

$$D_0 \simeq 2\delta \propto R_F \tag{11}$$

taking the "true" extension $\delta \simeq \delta_{tail}$ as in eq 2. This gives the simple relation

$$D_0 \propto N^{3/5} \tag{12}$$

(ii) For finite F^* considerable overlap may be necessary for any repulsive force to be detected, i.e.

$$D_0 \ll 2\delta \tag{13}$$

In this limit the *second* term in braces in eq 10 dominates, and we find

$$D \propto \delta^{1/2} \propto N^{3/10} \tag{14}$$

This approach suggests the distance of onset of interactions, measured in the surface forces experiments, should vary as

$$D \propto N^{\beta}$$

with $\beta = 0.3$–0.6. Over the range of parameters in our experiments we find an exponent $\beta \simeq 0.43$, consistent with these simple considerations.

The inequality in (13), together with the actual values of D_0 observed in our measurements, deserves comment. For example, for PEO of $M = 1.2 \times 10^6$ in water, the radius of gyration as evaluated from intrinsic viscosity data[3] (for the same Toyo Soda sample as used in our experiments) is 64 nm, from which the swollen end-to-end distance may be estimated as

$$R_F \simeq 6^{1/2} \times 64 \simeq 150 \text{ nm}$$

Taking the extension of tails from each surface as[19] (a conservative estimate)

$$\delta \simeq R_F$$

we have

$$2\delta = 2R_F \simeq 300 \text{ nm}$$

This compares with an interaction onset distance of

$$D_0 \simeq 190 \text{ nm}$$

for this polymer (Table I); i.e., this rather crude estimate is consistent with the limit suggested by the inequality (13) that there is appreciable overlap of the adsorbed layers prior to the detection of repulsion at $D = D_0$. This is also consistent with calculations by Scheutjens and Fleer,[20] which suggest that the extension of tails of adsorbed polymers from the adsorbing substrate is substantially greater than the unperturbed dimensions of the polymer.

To summarize: our force measurements provide a direct measure of the separation D_0 at which interaction between two surfaces bearing adsorbed polymer is first detectable. Within the range of experimental parameters in our studies we find (in good solvents)

$$D_0 \propto N^{0.43}$$

This is consistent with an analysis that assumes an extension

$$\delta \propto N^{3/5}$$

of the adsorbed layers from each adsorbing substrate and suggests appreciable overlap of the adsorbed layers before interaction is first detected with our apparatus.

It is of interest finally to consider the implication of our argument for Θ and poor solvents. In such systems one expects the polymer volume fraction a distance z from the surface to vary as

$$\phi(z) = \phi_s(a/z) \tag{15}$$

rather than as in eq 9 for good solvents.[15] For the case of Θ solvents there is some difficulty in interpreting the distance for onset of interactions, as the two-body interactions are compensated out in these conditions[18] (i.e., the second virial coefficient disappears). In this case the opposing segments essentially "telescope" freely into each other as the polymer-bearing surfaces approach (as has indeed been observed experimentally[21]) and *bridging attraction* due to polymers spanning the gap between the surfaces may be important[21] and interfere with the simple analysis applied to good solvents.

For the case of *poor* solvents, however, one may again expect initial interaction (in this case attractive) to commence at the point where osmotic *attraction* between opposing segments is first observed (in our apparatus) as the polymer-bearing surfaces approach. In this case the total attractive osmotic interaction due to overlap of segments in the "lens" (Figure 2) becomes

$$E(D) \simeq vV\phi_0^2kT/a^3 \tag{16}$$

rather than as in eq 6, where v is a negative second virial coefficient[18] ($v \simeq 0.1$–0.2 for the systems studied[10]). Carrying through the solution of eq 4, 5, 7, 8, 15, and 16 as for the good solvent case, we find

$$F^* = \frac{v\pi RkT\phi_s^2}{a^3}\left(\delta - \frac{D_0}{2}\right)\left(\frac{2a}{D_0}\right)^2\left\{1 + \frac{2}{D_0}\left(\delta - \frac{D}{2}\right)\right\} \tag{17}$$

which again has two limits: (i) For $F^* \to 0$ we expect forces to be measurable at little overlap of the opposing layers

$$D_0 \simeq 2\delta$$

but in this case the "true" extension δ may be taken as the *unperturbed* dimension R_0

$$\delta \simeq R_0 = aN^{1/2}$$

expected close to Θ conditions. This gives the simple dependence

$$D_0 \propto N^{1/2} \tag{18}$$

(ii) For finite F^* and considerable overlap before attraction is detected

$$D_0 \ll 2\delta$$

and in this limit we find

$$D_0 \propto \delta^{2/3} \propto N^{1/3} \tag{19}$$

The experimental data for poor solvents is less extensive than in the good solvent case. For the case of polystyrene in cyclohexane at $T < \Theta$ three molecular weights M have been studied,[10,22] $M = 10^5$, 6×10^5, and 9×10^5. The range of attractive interactions for these three polymers scales approximately as R_g, as shown in Figure 3, though there is more scatter in the data. This indicates that eq 18 rather than eq 19 may apply, i.e., that attractive interaction is detected at $D_0 \simeq 2\delta$ with little overlap of the opposing adsorbed layers. Now the thickness of the layers in poor solvents is substantially smaller (in terms of R_g) than for good solvents, while the total adsorbed amounts are comparable; thus the concentration of polymer segments near the cutoff (at δ) in the poor solvent is expected to be appreciably higher than in good solvents. In this case the polymer concentration in the "lens" (Figure 2) will be substantially greater on initial overlap in poor solvents, as will $E(D_0)$; this is consistent with detection of attractive forces soon after overlap ($D_0 \simeq 2\delta$) as indicated by the scaling of the experimental observations (Figure 3) with $N^{1/2}$ rather than with eq 19.

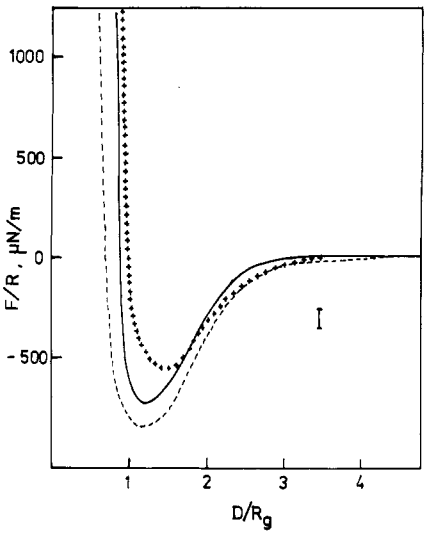

Figure 3. Force (F)–distance (D) profiles between curved mica surfaces (radius of curvature $R \simeq 1$ cm) bearing adsorbed polystyrene (molecular weight M) in cyclohexane in poor solvent conditions ($T < \Theta = 35$ °C). The distance axis is normalized with respect to the radii of gyration of the respective polymers, while the force axis is given as F/R, which normalizes the force profiles to interaction-energy profiles in the Derjaguin approximation.[10] (+) $M = 1 \times 10^5$, $T = 21$ °C, from ref 10 ($R_g = 8.5$ nm). (—) $M = 6 \times 10^5$, $T = 23$ °C, from ref 10 ($R_g = 21$ nm). (– – –) $M = 9 \times 10^5$, $T = 26$ °C, from ref 22 ($R_g = 25.7$ nm). Bar indicates scatter of experimental points.

Acknowledgment. We especially thank P. Pincus for a fruitful comment concerning the poor solvent case. J.K. holds the Herman Mark Professorial Chair in Polymer Physics.

Registry No. PEO, 25322-68-3; polystyrene, 9003-53-6.

References and Notes

(1) Vincent, B. *Adv. Colloid Interface Sci.* **1974**, *4*, 197.
(2) Garvey, M. J.; Tadros, Th. F.; Vincent, B. *J. Colloid Interface Sci.* **1974**, *49*, 57; **1976**, *55*, 440.
(3) Kawaguchi M.; Mikura, M.; Takahashi, A. *Macromolecules* **1984**, *17*, 2063.
(4) Kawaguchi, M.; Hayakawa, K.; Takahashi, A. *Macromolecules* **1983**, *16*, 631.
(5) Kawaguchi, M.; Takahashi, A. *Macromolecules* **1983**, *16*, 1465.
(6) Lyklema, J.; van Vliet, T. *Faraday Discuss. Chem. Soc.* **1978**, *65*, 25.
(7) Cain, F. W.; Otweill, R. H.; Smitham, J. B. *Faraday Discuss. Chem. Soc.* **1978**, *65*, 33.
(8) Barnett, K. G.; Cosgrove, T.; Vincent, B.; Burgess, A.; Crowley, T.; King, T. A.; Turner, J. D.; Tadros, Th. F. *Polymer* **1981**, *22*, 283.
(9) Cosgrove, T.; Crowley, T. L.; Vincent, B. In *Adsorption from Solution*; Rochester, C.; Ottewill, R. N., Eds.; Academic: London, 1983.
(10) Klein, J. *J. Chem. Soc., Faraday Trans. 1* **1983**, *79*, 99.

(11) Klein, J.; Luckham, P. F. *Macromolecules* **1984**, *17*, 1048.
(12) Klein, J.; Luckham P. F. *Nature (London)* **1984**, *308*, 836.
(13) Luckham, P. F.; Klein, J. *Macromolecules* **1985**, *18*, 721.
(14) Brandrup, J.; Immergut, E. H., Eds. *Polymer Handbook*; Wiley: New York, 1975.
(15) de Gennes, P.-G. *Macromolecules* **1981**, *14*, 1637; **1982**, *15*, 429.
(16) de Gennes, P.-G. *Scaling Concepts in Polymer Ppysics*; Cornell University Press: Ithaca, NY, 1979.
(17) The existence of anomalous scaling exponents very near the surface should not influence the present discussion: see, for example: de Gennes, P.-G.; Pincus, P. *J. Phys. Lett.* **1984**, *45*, L 953 and also Binder, K.; Kremer, K. *NATO Adv. Study Inst. Scaling in Disordered Systems*, in press.
(18) Flory, P. J. *Principles of Polymer Chemistry*; Cornell University Press: Ithaca, NY, 1953.
(19) Strictly speaking one should consider the effective "span" of the polymer: this is comparable with or slightly larger than R_0 in the unperturbed state—see: Rubin, R. J.; Mazur, J.; Weiss, G. H. *Pure Appl. Chem.* **1976**, *46*, 143. As this is an average value, in practice some segments will be extended considerably beyond this.
(20) Scheutjens, J. M. H. M.; Fleer, G. J. *Adv. Colloid Interface Sci.* **1982**, *16*, 341, 360; *Macromolecules* **1985**, *18*, 1882.
(21) Almog, Y.; Klein, J. *J. Colloid Interface Sci.* **1985**, *106*, 33.
(22) Israelachvili, J. N.; Tirrell, M.; Klein, J.; Almog, Y. *Macromolecules* **1984**, *17*, 204.

Craze Fibril Stability and Breakdown in Polystyrene

Arnold C.-M. Yang and Edward J. Kramer*

Department of Materials Science and Engineering and the Materials Science Center, Cornell University, Ithaca, New York 14853

Chia C. Kuo and S. Leigh Phoenix

Department of Mechanical and Aerospace Engineering and the Materials Science Center, Cornell University, Ithaca, New York 14853. *Received January 6, 1986*

ABSTRACT: Craze fibril stability of polymer glasses can be characterized by measuring the median strain (craze fibril stability) at the onset of craze fibril breakdown in thin films under a constant low strain rate. Monodisperse polystyrenes (PS's) of molecular weight M = 37 000–20 000 000 were used. A strong increase in craze fibril stability was found as M increased from 50 000 to 200 000. The increase occurred over the same range as the increase in macroscopic fracture toughness of PS. Voids were observed to always nucleate at the bulk–craze interface and never in the craze midrib. Higher strain rates reduced the craze fibril stability. Foreign particle inclusions, e.g., dust, in specimens can significantly decrease the fibril stability from its intrinsic (clean) value. Even in the presence of such particles, however, the M dependence of fibril stability is qualitatively similar to that of crazes in "dust-free" films. The fibril breakdown statistics can be investigated by examining simultaneously the failure events in a large number of independent film specimens. The statistics of craze fibril breakdown are found to follow a Weibull distribution. Two parameters may be extracted by fitting this distribution to the breakdown data: (1) a Weibull scale parameter ϵ_W, which is a measure of craze fibril stability, and (2) a Weibull modulus ρ, which is a measure of variability, that is, the breadth of the distribution of fibril stability (high ρ's produce narrow distributions and vice versa). The Weibull distribution in a weakest-link setting can be used to predict the effect of sample size on the probability of craze fibril breakdown somewhere in the sample. A microscopic statistical model in which craze fibrils fail by random disentanglement of molecular strands at the craze–bulk interface is developed. The experimental observations are in good agreement with the predictions of the model.

Introduction

The brittle fracture commonly observed in many glassy polymers under tension can be traced to the formation and breakdown of crazes, localized microdeformation zones composed of many aligned fibrils.[1-4] The fibrils are drawn from a narrow layer of strain-softened polymer on the bulk polymer–craze interfaces. As initially drawn the fibrils are usually strongly load-bearing and bridge between these two interfaces. It is observed, however, that craze fibrils can break down to form large voids which are the first stage in catastrophic fracture.[5-7] Thus the mechanisms of fibril breakdown are of crucial importance in the study of the fracture properties of these matterials.

Previous work on craze fibril stability has focused primarily on theoretical description and indirect measurements in poly(methyl methacrylate) (PMMA). Verheulpen-Heymans[8] explored theoretically craze failure in PMMA by assuming that fibrils fail by disentanglement of chains in the midrib, the layer of fibrils in the center of the craze. This fibrillar material forms just behind the craze tip and thus is the oldest region of the craze. Schirrer and co-workers[9,10] have inferred a "disentanglement time" involved in such failure of craze fibrils in PMMA by observing the craze–crack optical thickness profiles by interference optical microscopy. However, to understand the craze fibril breakdown mechanisms we first must be able to measure the onset of such breakdown directly. In this paper, we introduce a simple test from which the fibril stability and the fibril breakdown statistics can be determined. This test will enable us to explore the mechanisms of fibril breakdown and the molecular factors controlling the craze fibril stability.

Experimental Procedures

Thin films of monodisperse polystyrene (PS) ($M_w/M_n < 1.3$) were prepared from polymer of molecular weight M = 37 000, 50 000, 110 000, 233 000, 390 000, 900 000, 1 800 000, and 20 000 000 purchased from Pressure Chemical Co. The PS was dissolved in toluene, and uniform thin films were formed by drawing glass microscope slides from the solution at a constant speed. The film thickness was measured with a Zeiss interference microscope and was held constant at 0.4 μm. After the solution had escaped, the film was floated off the slide onto the surface of a water bath, and subsequently picked up on a ductile copper grid. The bars of this grid had previously been coated with a thin layer of PS by dipping the copper grid into a PS solution. A brief exposure to toluene vapor removed any slack in the film and served to bond the film to the copper grid.[11] This process enables each of the

0024-9297/86/2219-2010$01.50/0